Carbohydrate Polymers 78 (2009) 36–40

Contents lists available at ScienceDirect

Carbohydrate Polymers

journal homepage: www.elsevier.com/locate/carbpol

# Protonation behavior of cotton fabric with irreversibly adsorbed chitosan: A potentiometric titration study

Duško Čakara [a,*], Lidija Fras [b], Matej Bračič [b], Karin Stana Kleinschek [b]

[a] Department of Biotechnology, University in Rijeka, Trg Braće Mažuranića 10, 51000 Rijeka, Croatia
[b] Laboratory for Characterization and Processing of Polymers, Faculty of Mechanical Engineering, University of Maribor, Smetanova 17, SI-2000 Maribor, Slovenia

ARTICLE INFO

*Article history:*
Received 10 October 2008
Received in revised form 15 April 2009
Accepted 17 April 2009
Available online 3 May 2009

*Keywords:*
Chitosan
Cotton
Protonation
Adsorption
Charge
pH
p*K*
Titration
Potentiometric
Medical
Antimicrobial

ABSTRACT

The protonation of cotton fabric with irreversibly adsorbed medical chitosan (CO–CT) was measured in aquatic medium at 0.1 M ionic strength by means of potentiometric titrations, and compared with the results obtained for pure cotton and chitosan. For CO–CT, the charging isotherm exhibits a charge reversal around pH $\approx$ 6.0, which is identified as the point of zero charge (PZC). The pure chitosan and the acid fraction that is present in cotton, protonate according to the one-p*K* model, with $\mathrm{p}K_{\mathrm{CT}} = 6.3$ and $\mathrm{p}K_{\mathrm{CO}} = 4.7$, respectively. At pH > PZC, the charge of the acid fraction in CO–CT is negative and constant, and the proton binding is attributed purely to the adsorbed chitosan. On the other hand, the cotton-bound acid exhibits a more complex protonation mechanism in CO–CT than in the pure fabric, which is evidenced as an excess positive charge at pH < PZC and a deviation from the one-p*K* behavior.

## 1. Introduction

Chitosan is a cationic polysaccharide produced by the deacetylation of chitin (Steinbüchel, Vandamme, De Baets, & Steinbüchel, 2002). The low production costs and biocompatibility make chitosan an attractive material for food processing (Devlieghere, Vermeulen, & Debevere, 2004; Shahidi, Arachchi, & Jeon, 1999), biomedical applications (Berger et al., 2004; Issa et al., 2006) and water purification (Babel & Kurniawan, 2003; Bailey, Olin, Bricka, & Adrian, 1999), just to mention a few. Due to the glucosamine monomer unit, chitosan is chemically compatible with a vast number of polysaccharides, in particular with cellulose (Li & Bai, 2005; Maciel, Silva, Paula, & de Paula, 2005; Pascual & Julir, 2001). It adsorbs irreversibly to cotton fibers, in sufficient concentrations for a pronounced antimicrobial activity (Helander, Nurmiaho-Lassila, Ahvenainen, Rhoades, & Roller, 2001; Rabea, Badawy, Stevens, Smagghe, & Steurbaut, 2003).

The mechanisms by which chitosan adheres to microbial membranes, complexates heavy metals and interacts with other (poly)-ions, involve the protonation of the primary amine groups (Guzman, Saucedo, Navarro, Revilla, & Guibal, 2002; Jin & Bai, 2002; Rabea et al., 2003; Sogias, Williams, & Khutoryanskiy, 2008). Thus, most of the useful properties of chitosan depend on its degrees of deacetylation and protonation. The subject of the present study is the pH-dependent protonation behavior of chitosan, irreversibly adsorbed onto cotton fibers that exhibit a non-negligible anionic character, due to the presence of an acid fraction (Herrington & Midmore, 1984a, 1984b;Stana-Kleinschek & Ribitsch, 1998; Steinbüchel et al., 2002). The latter could not be removed by washing or ion exchange, and is most probably present as covalently bound carboxyl groups. The influence of the electrostatic interactions between cotton and chitosan on the overall charging isotherm will be examined, and related to the adsorption mechanism. The timescale and reversibility of the proton binding is compared for the cotton fabric in the presence and absence of chitosan.

## 2. Experimental

### 2.1. Materials

The cotton fabric used in this study was produced by Lenzing Ag, Austria. The linear density of the fibers equals 1.3 dtex

---

[*] Corresponding author. Tel.: +385 51 651 274; fax: +385 51 651 135.
*E-mail address:* dusko.cakara@medri.hr (D. Čakara).

0144-8617/$ - see front matter © 2009 Elsevier Ltd. All rights reserved.
doi:10.1016/j.carbpol.2009.04.011

(dg/km) and the fiber length 39 mm. Before titration, the fabric was demineralized by washing in deionized water until the conductivity in the surrounding bath was lower than 3 μS/cm. The fabric was then air dried and stored at standard atmosphere conditions ($T = 293 \pm 2$ K and relative humidity 65 ± 2%).

The medical grade chitosan with a high degree of deacetylation was kindly supplied by Gillet Chitosan, France. The molecular weight of the sample is ca. 300 kDa (kg/mol), determined by the manufacturer from the viscosity measurements. The total organic carbon and total nitrogen (TOC/TN) content in the samples was measured by means of the Analytik Jena Multi C/N 2100 instrument, and was found to conform with the formula and the degree of deacetylation $dd \approx 98\%$. In order to prepare the impregnation solution, 1 g of dry chitosan powder was added to 100 mL of water at 40 °C and pH ≈ 3.6, set by adding concentrated acetic acid, and dissolved under vigorous stirring for ca. 2 h.

The adsorption of chitosan was achieved by impregnating the fabric with the chitosan solution ($x = 1\%$) in a double-wheel press, after which the impregnated fabric was left to dry. Subsequently, the reversibly adsorbed chitosan was removed by washing the fabric for 2 h in 1 mM HCl and 1 mM KOH, followed by deionization in pure water until a constant conductivity of 3 μS/cm was achieved.

### 2.2. Potentiometric titrations

A two-burette instrument (Mettler T-70) was used, equipped with a combined glass electrode (Mettler T DG 117). The burettes were filled with 0.1 M HCl (Merck, Titrisol) and 0.1 M KOH (Baker, Dilut-it). All the solutions were prepared with deionized water with a very low carbonate content ($< 10^{-6}$ M), which was achieved through boiling and subsequent cooling under nitrogen atmosphere.

The pure chitosan solution ($x = 1\%$), the non-impregnated and the impregnated cotton fabrics ($m_f = 5$ g), were all titrated in several forth and back runs between pH 3 and 11. In order to avoid sticking to the electrode and jamming with the stirrer, the fabric was kept in a stainless steel tea container. Prior to the titrations, the ionic strength was set to 0.1 M by adding pure solid KCl (Kemika, Zagreb). The variation of the ionic strength upon additions of HCl and KOH remains within 2% of the initial value, thus very nearly constant. The blank HCl–KOH titrations were performed under the same conditions as mentioned above.

The electrode readings were recorded either after a drift of < 0.1 mV/min or a maximum waiting time condition was satisfied. In the case of pure chitosan and cotton fabric, the equilibrium reading was achieved within max. 3 min. In the case of CO–CT, the waiting time to reach equilibrium was found to be much longer. The origin of this occurrence was investigated in a set of experiments, where the maximum waiting time was varied, up to 12 min.

The molar concentration $Q$ related to the overall charge of the weak ions, was calculated from the charge balance equation

$$Q = \sum_i c_i z_i = [\mathrm{OH}^-] - [\mathrm{H}^+] + [\mathrm{Cl}^-] - [\mathrm{K}^+], \qquad (1)$$

where square brackets and $c_i$ denote molar concentrations of ionic species, and $z_i$ is the charge number of the species i. The concentrations $[\mathrm{K}^+]$ and $[\mathrm{Cl}^-]$ are calculated from the added volumes and concentrations of the burette solutions. The proton and hydroxide ion concentrations were calculated from the pH reading as $[\mathrm{H}^+] = c^\circ \cdot 10^{-\mathrm{pH}}/\overline{\gamma}_\pm$ and $[\mathrm{OH}^-] = c^\circ \cdot 10^{(\mathrm{pH}-\mathrm{p}K_\mathrm{w})}/\overline{\gamma}_\pm$, where $\overline{\gamma}_\pm$ is the average activity coefficient of the singly charged ions, calculated from the Davies formula (Stumm & Morgan, 1996), p$K_\mathrm{w}$ is the negative logarithm of the ionic product of water and $c^\circ = 1\ \mathrm{mol\,dm}^{-3}$. In order to eliminate the variation of $Q$ due to the dilution of the titrated solution upon titrant additions, it is most convenient to report the charging isotherm in the form of $QV_t$(pH), $V_t$ being the volume of the titrated solution at each stage of the experiment. The product $QV_t$(pH) should be interpreted as the charge present in the system due to the weak ions, in units of moles of elementary charges.

## 3. Results

The resulting charging isotherms $QV_t/m_f$ vs. pH, are presented in Fig. 1. The figure contains titration data for three different samples, namely the pure cotton fabric (CO, squares), pure chitosan (CT, triangles), and the cotton fabric with irreversibly adsorbed chitosan (CO–CT, circles). In the case of CO and CO–CT, the presented charge is attributed to the charge of the fabric-bound weakly acidic or basic species, determined by the proton-binding equilibrium. For these samples a parallel can be drawn between $QV_t/m_f$ and the surface charge $\sigma = QV_t/A$, that is usually reported for colloidal particles, and where $A$ is the surface area of the particles. However, the surface of a fabric is not exactly defined, and therefore the term "surface charge" is avoided within the present article. The isotherms are rather normalized with the mass of the fabric $m_f = 5$ g in order to facilitate data comparison among all of the presented samples. Thus in the case of CT, even though the fabric is not actually present in the sample, the charge is normalized with the mass of the fabric present in the CO and CO–CT experiments.

The isotherm of the pure cotton (cf. Fig. 1, squares) exhibits negative charge with a plateau at ca. −20 μmol per gram fabric, which is present at pH ≳ 6.0. On the other hand, the pure chitosan (cf. Fig. 1, triangles) exhibits positive charge, with a plateau at ca. 25 μmol per gram fabric that occurs at pH ≲ 5.0. In the case of CO–CT (cf. Fig. 1, circles), the charge is positive at low pH and negative at high pH, with a reversal that occurs at pH = 6.0. The pH value of the charge reversal is identified as the point of zero charge (PZC). The total titratable charge in the case of CO–CT, calculated as the difference between the two plateau values of the isotherm, amounts to ca. 45 μmol elementary charges per gram fabric. The buffering region, in which the proton exchange between the CO–CT system and the bulk solution occurs, lies in the range 4.5 ≲ pH ≲ 7.0.

In the case of CO–CT, the reported charge can be attributed to the amine groups of the irreversibly adsorbed chitosan, and the covalently bound carboxyl groups present in cotton, since the

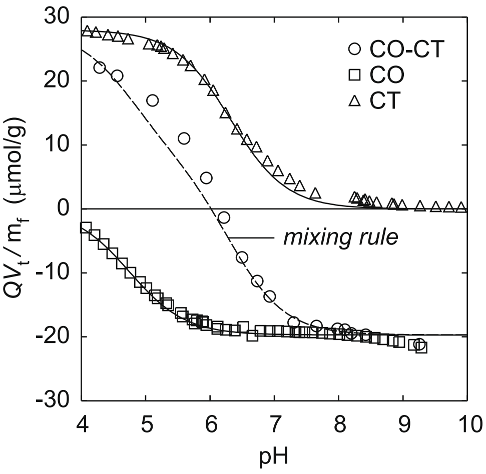

**Fig. 1.** Charging isotherms of the pure chitosan (CT), pure cotton fabric (CO) and cotton fabric in the presence of adsorbed chitosan (CO–CT), measured at $I = 100$ mM. The charge amount $QV_t$ is normalized with the mass od the fabric $m_f$ (see text). Solid lines represent the one-p$K$ model with p$K_\mathrm{CO} = 4.7$ and p$K_\mathrm{CT} = 6.3$. Dashed curve is the sum of the solid curves, according to the "mixing rule".

reversibly bound chitosan was removed by washing the fabric prior to the titration experiment. The titrations of the solution after removing the fabric exhibited a negative charge of ca. 1 μmol elementary charges per gram fabric above pH $\approx$ 6.5 (not shown). The CO–CT isotherm was corrected for the latter minor charge, which should be attributed to the dissolved carbonic acid. The total organic carbon/total nitrogen (TOC/TN) analysis of the titration solution after removing the fabric, showed a detectable, however, negligibly low presence of chitosan in the bulk solution of ca. 15 mg dm$^{-3}$, corroborating the absence of chitosan desorption during the potentiometric titration experiment.

The solid lines in Fig. 1 represent the best-fit one-p*K* model isotherms described by equation

$$\mathrm{pH} = \mathrm{p}K - \log\left(\frac{\theta}{1-\theta}\right) \tag{2}$$

where $\theta$ represents the degree of protonation which was obtained from the plateau values $Q_{\max}V_{\mathrm{t,\,max}}$ and $Q_{\min}V_{\mathrm{t,min}}$ of the isotherms as

$$\theta = \frac{QV_{\mathrm{t}} - Q_{\min}V_{\mathrm{t,min}}}{Q_{\max}V_{\mathrm{t,max}} - Q_{\min}V_{\mathrm{t,min}}} \tag{3}$$

while p*K* is the deprotonation equilibrium constant. In the present case, the best-fit for cotton and chitosan was obtained with values $\mathrm{p}K_{\mathrm{CO}} = 4.7$ and $\mathrm{p}K_{\mathrm{CT}} = 6.3$, respectively. It can be observed the one-p*K* model satisfactorily describes the experimental data for both samples. For chitosan, the obtained p*K* value is in a very good agreement with other authors findings (Wang et al., 2006), while for cotton, it is slightly higher than expected (Fras et al., 2004; Herrington & Midmore, 1984a).

The dashed line in Fig. 1 is the so called *mixing rule* isotherm, which is obtained by summing up the charges of the separate components (solid lines) (Cakara, Chassagne, Gehin-Delval, & Borkovec, 2007; Čakara, Kobayashi, Skarba, & Borkovec, 2009; Vermeer & Koopal, 1999). It is therefore equivalent to a two-step charging isotherm with $\mathrm{p}K_1 = 4.7$ and $\mathrm{p}K_2 = 6.3$, and the plateaus that correspond to the amounts of the surface-bound acid and the adsorbed chitosan present in the CO–CT system. It can be observed that the mixing rule very well describes the experimental CO–CT charging isotherm above the PZC, while the fit is less satisfactory below the PZC. These observations will be discussed below.

The timescale and the reversibility of the proton binding for CO–CT is reported in Fig. 2. Here, several forth-back titration runs were performed under varied waiting times for data acquisition. For the experiment where the maximum waiting time was set to 3 min (dotted line), a broad hysteresis and significant data scattering is observed. Under same conditions, a perfectly reversible isotherm was observed for pure cotton (not shown). The scattering becomes less pronounced as the waiting time is increased (dashed line), however, the hysteresis disappears only if the waiting time is increased to > 12 min per reading (solid line).

Fig. 3 presents the proton-binding isotherms in the light of the effective p*K* defined as

$$\mathrm{p}K_{\mathrm{eff}} = \mathrm{pH} + \log\left(\frac{\theta}{1-\theta}\right) \tag{4}$$

In order to calculate $\mathrm{p}K_{\mathrm{eff}}$, the overall degree of protonation ($\theta$) in the mixed system was calculated from the CO–CT isotherm by using Eq. (3). The significance of $\mathrm{p}K_{\mathrm{eff}}$ should not be confused with the p*K* in Eq. (2). The former is a function of $\theta$, which will be discussed below, while the latter is a thermodynamic equilibrium constant.

## 4. Discussion

The anionic character of the fabric may be attributed to the presence of an irreversibly bound acid fraction, which is common for the industrial cotton and depends on the production technology (Fras et al., 2004; Herrington & Midmore, 1984a, 1984b; Steinbüchel et al., 2002). In the present case, the value $\mathrm{p}K_{\mathrm{CO}} = 4.7$ is moderately higher than expected for oxycellulose (p*K* $\approx$ 4.2) and considerably higher than expected for uronic acids (p*K* $\approx$ 3.5) (Fras et al., 2004; Herrington & Midmore, 1984a). Since the protonation of the pure fabric follows an one-p*K* model, we speculate that the negative charge can be attributed to a single acid compound, probably oxycellulose. Consequently, the higher p*K*-value is probably caused by a less hydrophilic environment in the fiber interior.

Let us now address the origin of the force which drives the irreversible adsorption of chitosan in the CO–CT system, and which is implicated in the charging isotherm. The maximum positive charge of the adsorbed chitosan, inferred from the plateau at low pH in Fig. 1, roughly equals the maximum negative charge of cotton inferred from the plateau at high pH. Intuitively, this points to the formation of an electrostatically stabilized (poly)ionic complex. However, a closer insight is gained by comparing the CO—CT data with the mixing rule protonation isotherm. The latter describes

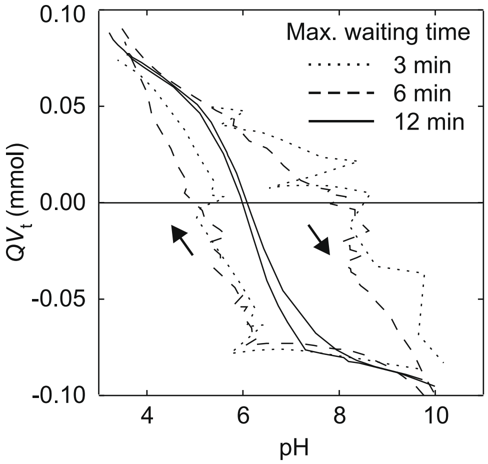

**Fig. 2.** Charging curves of the cotton fabric in the presence of adsorbed chitosan, measured in forward–backward potentiometric titrations at $I = 100$ mM and at varied pH-sweep rates. The mass of the titrated fabric with adsorbed chitosan is 5 g.

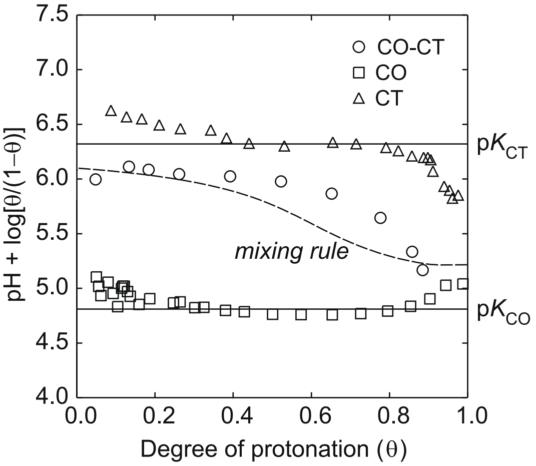

**Fig. 3.** Effective p*K* (cf. Eq. (4)) as function of the degree of protonation for the pure chitosan, pure cotton fabric, and the cotton fabric with adsorbed chitosan, as calculated from the data presented in Fig. 1. Solid lines represent the one-p*K* model, while the dashed curve is calculated from the sum of the one-p*K* isotherms (see Fig. 1).

one of the three possible regimes in which the net charge is not altered upon adsorption, as illustrated in Fig. 4. In the first regime, the protonation states of both phases are not altered upon adsorption (cf. Fig. 4a). This would occur for example in complexes between strongly acidic and strongly basic polyelectrolytes or surfaces, irrespectively of the presence of electrostatic interactions. However, in the case of weak polyions, the electrostatic interactions would favor increased partial charges. Thus, in the case of the CO–CT system, the first regime would implicate an absence of electrostatic interactions. In the second regime, the excess protonation of one phase is exactly matched by the deprotonation of the other, which leads to increased partial charges, but does not affect the net sum (cf. Fig. 4b). This is the regime expected for an electrostatically stabilized complex between a weakly acidic and a weakly basic polyelectrolyte or surface, such as CO–CT. The third regime is similar, but with a decrease of partial charges, which can for example occur if the adsorption leads to a more hydrophobic environment for the weakly acidic and basic groups (cf. Fig. 4c).

The experimental data for CO–CT in Fig. 1 conform with the mixing rule in the pH-range above the PZC ($\mathrm{pH} \geqslant 6.0$), which allows us to assess one of the above described regimes. The adjustment of the partial charges is possible within the buffering pH regions, thus for chitosan roughly within $5.0 \lesssim \mathrm{pH} \lesssim 8.0$, and for cotton within $\mathrm{pH} \lesssim 6.0$ (cf. Fig. 1). Within the overlap of these two ranges $5.0 \lesssim \mathrm{pH} \lesssim 6.0$, the mixing rule isotherm could be assigned to any of the above mentioned mechanisms. However, should the electrostatic interaction be involved, the partial charge of chitosan would be increased within $6.0 \lesssim \mathrm{pH} \lesssim 8.0$. The agreement of the data with the mixing rule in the latter range shows that the partial charge of chitosan is not affected by the presence of the oppositely charged cotton, which in turn unambiguously points to the first mechanism (cf. Fig. 4a). Thus, it can be concluded that for the CO–CT system, the adsorption is not, or at least not predominately, driven by electrostatic interactions. This is not surprising having in mind the relatively high ionic strength, under which conditions the electrostatic interactions are largely screened by the counterions.

At $5.0 < \mathrm{pH} < \mathrm{PZC}$ the measured charge is moderately more positive than the mixing rule prediction, pointing to an excess protonation in the presence of adsorption. As discussed above, the partial charge of chitosan seems not to be affected by the adsorption, in which case the excess protonation should be attributed to cotton. A tentative explanation for such behavior of cotton in the presence of adsorbed chitosan is gained from the reversibility experiments shown in Fig. 2. In the experiment where the waiting time between the two successive titration points was set to 3 min (dotted line), a broad hysteresis between the forth and back titration runs is observed. When the waiting time is increased to 12 min (solid line), the hysteresis, caused by a slow establishment of the proton-binding equilibrium, almost disappears. On the other hand, the hysteresis was not observed in the case of pure cotton, pointing to a much faster establishment of the proton-binding equilibrium in that case. A possible explanation is that the adsorbed chitosan compacts the fiber surface and thereby reduces the hydration of the fiber interior, where the largest portion of the cotton-bound acid is found. In turn, the protonation equilibrium of the weakly acidic groups shifts in favor of the protonated form, which is the origin of the observed increased net positive charge.

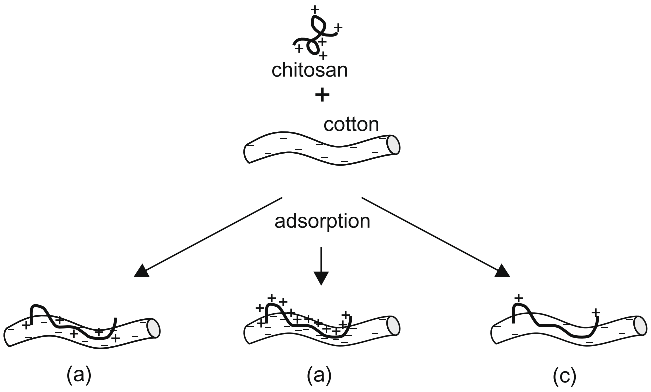

**Fig. 4.** Charging regimes upon adsorption, which can result with the "mixing rule" isotherm: (a) the partial charges of the components are conserved upon adsorption; (b) the partial charges increase by the same amount; (c) the partial charges decrease by the same amount.

The non-electrostatic origin of the adsorption is also corroborated by the isotherms presented in Fig. 3. This representation of the charging isotherms actually reflects the protonation free energy, which can be written as:

$$\Delta_{\mathrm{r}}G = -2.303kT\{\mathrm{pH} + \log[\theta/(1-\theta)]\} + \Delta G_{\mathrm{el}} \qquad (5)$$

where $\Delta G_{\mathrm{el}}$ denotes the electrostatic term. The latter is a function of the charge density at the polyelectrolyte or surface, and can be written in terms of the surface potential $\psi_0$ as $\Delta G_{\mathrm{el}} = e\psi_0(\theta)$, where $e$ denotes the elementary charge (Borkovec, Jönsson, & Koper, 2001, Tanford, 1961). The term within the braces in Eq. (5) is the effective deprotonation equilibrium constant, p$K_{\mathrm{eff}}$. The solid lines in Fig. 3 represent the one-p$K$ isotherms, for which $\Delta G_{\mathrm{el}} = 0$, while the dashed line represents the mixing rule isotherm. As $\theta \to 0$, the cotton-bound acid becomes completely deprotonated while p$K_{\mathrm{eff}}$ observed for CO–CT becomes moderately lower than p$K_{\mathrm{CT}}$, indicating a promoted deprotonation of chitosan. Conversely, as $\theta \to 1$, the observed p$K_{\mathrm{eff}}$ becomes moderately higher than p$K_{\mathrm{CO}}$, indicating a promoted protonation of the cotton-bound acid. Both of these observations point to the fact that the electrostatic attraction, if present at all, is not the dominant driving force for the adsorption. Otherwise, the formation of the charged species would be promoted, thus evidenced as $\mathrm{p}K_{\mathrm{eff}} > \mathrm{p}K_{\mathrm{CT}}$ at $\theta \to 0$ and $\mathrm{p}K_{\mathrm{eff}} < \mathrm{p}K_{\mathrm{CO}}$ at $\theta \to 1$. The smooth decrease of p$K_{\mathrm{eff}}$ as $\theta$ becomes larger than 0.4, and approaching p$K_{\mathrm{CO}}$ as $\theta \to 1$, is a consequence of a simultaneous protonation of both components. Thus, in spite of the fact that both chitosan and the cotton-bound acid occur in a large pH-range as oppositely charged species, the electrostatic attractions between these two fractions are under present conditions absent due to the screening by counterions.

## 5. Conclusion

The charging isotherms of both chitosan and cotton follow an one-p$K$ model. The weakly acidic cotton fabric irreversibly binds chitosan with a roughly 1:1 ratio of amine to carboxyl groups, and the composite system exhibits a point of zero charge around $\mathrm{pH} \approx 6$. However, at 0.1 M ionic strength, the comparison of the overall charging isotherm with the sum of the isotherms of the pure components, reveals an absence of the electrostatic attraction between cotton and chitosan. This is also evidenced from the effective p$K$ value of the composite. Thus, the irreversible adsorption of chitosan onto the weakly acidic cotton fabric is under present conditions predominately driven by a non-electrostatic attraction.

## Acknowledgements

We thank Mr. Dominique Gillet of the Gillet Chitosan France company for the kind supply of medical chitosan. We further thank Vida Žižek and Tanja Kos from the LCPP, Faculty of Mechanical Engineering, University in Maribor. This research project has been supported by a Marie Curie Transfer of Knowledge Fellowship of the EC's 6 FP under contract no. MTKD-CT-2005-029540-POLYSURF.

## References

Babel, S., & Kurniawan, T. A. (2003). Low-cost adsorbents for heavy metals uptake from contaminated water: A review. *Journal of Hazardous Materials, 97*(1–3), 219–243.

Bailey, S. E., Olin, T. J., Bricka, R. M., & Adrian, D. D. (1999). A review of potentially low-cost sorbents for heavy metals. *Water Research, 33*(11), 2469–2479.

Berger, J., Reist, M., Mayer, J. M., Felt, O., Peppas, N. A., & Gurny, R. (2004). Structure and interactions in covalently and ionically crosslinked chitosan hydrogels for biomedical applications. *European Journal of Pharmaceutics and Biopharmaceutics, 57*(1), 19–34.

Borkovec, M., Jönsson, B. J. M., & Koper, G. J. M. (2001). Ionization processes and proton binding in polyprotic systems: Small molecules, proteins, interfaces and polyelectrolytes. In E. Matijević (Ed.), *Surface and colloid science* (Vol. 16). Plenum Publishing Corporation.

Cakara, D., Chassagne, C., Gehin-Delval, C., & Borkovec, M. (2007). Protonation of carboxyl latex particles in the presence of a strong cationic polyelectrolyte. *Colloids and Surfaces A: Physicochemical and Engineering Aspects, 294*(1–3), 174–180.

Čakara, D., Kobayashi, M., Skarba, M., & Borkovec, M. (2009). Protonation of silica particles in the presence of a strong cationic polyelectrolyte. *Colloids and Surfaces A: Physicochemical and Engineering Aspects, 339*(1–3), 20–25.

Devlieghere, F., Vermeulen, A., & Debevere, J. (2004). Chitosan: Antimicrobial activity, interactions with food components and applicability as a coating on fruit and vegetables. *Food Microbiology, 21*(6), 703–714.

Fras, L., Laine, J., Stenius, P., Stana-Kleinschek, K., Ribitsch, V., & Dolecek, V. (2004). Determination of dissociable groups in natural and regenerated cellulose fibers by different titration methods. *Journal of Applied Polymer Science, 92*(5), 3186–3195.

Guzman, J., Saucedo, I., Navarro, R., Revilla, J., & Guibal, E. (2002). Vanadium interactions with chitosan: Influence of polymer protonation and metal speciation. *Langmuir, 18*(5), 1567–1573.

Helander, I. M., Nurmiaho-Lassila, E. L., Ahvenainen, R., Rhoades, J., & Roller, S. (2001). Chitosan disrupts the barrier properties of the outer membrane of Gram-negative bacteria. *International Journal of Food Microbiology, 71*(2–3), 235–244.

Herrington, T., & Midmore, B. R. (1984a). Adsorption of ions at the cellulose/aqueous electrolyte interface. Part I. *Journal of the Chemical Society, Faraday Transactions I, 80*, 1525–1537.

Herrington, T., & Midmore, B. R. (1984b). Adsorption of ions at the cellulose/aqueous electrolyte interface. Part II. *Journal of the Chemical Society, Faraday Transactions I, 80*, 1539–1552.

Issa, M. M., Köping-Högglrd, M., Trmmeraas, K., Vlrum, K. M., Christensen, B. E., Strand, S. P., et al. (2006). Targeted gene delivery with trisaccharide-substituted chitosan oligomers in vitro and after lung administration in vivo. *Journal of Controlled Release, 115*(1), 103–112.

Jin, L., & Bai, R. (2002). Mechanisms of lead adsorption on chitosan/PVA hydrogel beads. *Langmuir, 18*(25), 9765–9770.

Li, N., & Bai, R. B. (2005). Copper adsorption on chitosan-cellulose hydrogel beads: Behaviors and mechanisms. *Separation and Purification Technology, 42*(3), 237–247.

Maciel, J. S., Silva, D. A., Paula, H. C. B., & de Paula, R. C. M. (2005). Chitosan/carboxymethyl cashew gum polyelectrolyte complex: Synthesis and thermal stability. *European Polymer Journal, 41*(11), 2726–2733.

Pascual, E., & Julir, M. R. (2001). The role of chitosan in wool finishing. *Journal of Biotechnology, 89*(2–3), 289–296.

Rabea, E. I., Badawy, M. E. T., Stevens, C. V., Smagghe, G., & Steurbaut, W. (2003). Chitosan as antimicrobial agent: Applications and mode of action. *Biomacromolecules, 4*(6), 1457–1465.

Shahidi, F., Arachchi, J. K. V., & Jeon, Y. J. (1999). Food applications of chitin and chitosans. *Trends in Food Science & Technology, 10*(2), 37–51.

Sogias, I. A., Williams, A. C., & Khutoryanskiy, V. V. (2008). Why is chitosan mucoadhesive? *Biomacromolecules, 9*(7), 1837–1842.

Stana-Kleinschek, K., & Ribitsch, V. (1998). Electrokinetic properties of processed cellulose fibers. *Colloids and Surfaces A: Physicochemical and Engineering Aspects, 140*(1–3), 127–138.

Steinbüchel, A., Vandamme, E. J., De Baets, S., & Steinbüchel, E. (2002). Biopolymers. Polysaccharides II Polysaccharides from Eukaryotes (Vol. 6). Wiley-VCH.

Stumm, W., & Morgan, J. J. (1996). *Aquatic chemistry* (3rd ed.). New York: John Wiley and Sons.

Tanford, C. (1961). *Physical chemistry of macromolecules*. New York: Wiley.

Vermeer, A. W. P., & Koopal, L. K. (1999). Charge adjustments upon adsorption of a weak polyelectrolyte to a mineral oxide: The HematiteHumic acid system. *Journal of Colloid and Interface Science, 212*(1), 176–185.

Wang, Q. Z., Chen, X. G., Liu, N., Wang, S. X., Liu, C. S., Meng, X. H., et al. (2006). Protonation constants of chitosan with different molecular weight and degree of deacetylation. *Carbohydrate Polymers, 65*(2), 194–201.